Optimization of Radial Fin Tubes Heat Exchanger with Minor Rectangular Annular Fins

Achmad Aminudin[1], Farid Majedi[2]

[1,2]Engineering Department, Politeknik Negeri Madiun (PNM), Jl. Serayu no 84, Madiun, Indonesia-63133

Abstract— *Radial fin tubes heat exchanger (HE) is a tool applied to transfer heat generated from the energy dissipation of an electronic equipment or heat exchanger. Increased heat transfer in this tool continues to be developed using fin disturbance. Therefore, this study evaluated minor rectangular annular fins (MRAFs) as extended surfaces in radial fin tubes that have the potential to increase flow turbulence intensity and convective heat transfer coefficient.*
3-D numerical analysis using Computational Fluids Dynamic (CFD) code Fluent is performed to obtain flow characteristics and heat transfer in HE radial fin tubes with MRAFs. The fin optimized parameters are the thickness and height of the MRAFs with constant Re_D. While the optimal combination identification is determined is the highest heat transfer value of each variation.
The results showed that by changing the dimensions of thickness and height MRFAs can increase the intensity of turbulent flow and convective heat transfer coefficient. However, the gap between fins with MRFAs shows the smaller Nusselt number. This is because the flow of freestream is hampered by secondary flow separation. The optimal combination is obtained on a 5 mm height variation with 1.5 mm thickness.

Keywords— *Optimization, numerical study, radial fin tube heat exchanger, and MRAFs.*

I. INTRODUCTION

Radial fin tubes heat exchangers are a tool applied to transfer heat from energy dissipation in an equipment. It can be applied to cooling electric component, air-cooled engine, and water heater in power plant and domestic. For its application, the outer surface of the tube is added to the extended surface of a radial plate arranged in parallel with the aim of increasing the water side heat transfer performance of the heat exchanger (HE).

Kim examined thermal optimization on branched-fin heat sinks on plates with water-cooled fluids using the Volume Averaging Theory (VAT) method [1]. The results concluded that the use of Y-shaped fin heat sink can reduce thermal resistance by 30% compared to rectangular fin heat sink. Shafeie et al. conducted a laminar forced convection numerical study on Microchannel Heat Sinks (MCHSs) and Pin Fin Heat Sinks (PFHSs) [2]. The results show that the use of MCHSs is able to increase heat transfer greater than with PFHSs. This is because the intensity of turbulent flow through the channel increases compared to PFHSs. The study was supported by Ahmed who added ribbed flats to the HSs plates [3]. Secondary flow phenomenon behind ribbed flat oscillating continuously can reduce thermal boundary layer on the plate surface. This impacts on the reduction of thermal resistance on the surface of the plate caused by the laminar boundary layer [4].

From the literature review that has been done, it can be identified that the thermal resistance caused by the laminar boundary layer on the surface of the tube generally has a dominant role in the reduction of heat transfer performance of the tube heat exchanger. Therefore, in this research will be optimized the use of radial fin with minor rectangular annular fins (MRAFs) as disturbance flow.

This study aims to identify the effect of MRAFs on radial fin-tube heat exchanger on flow characteristics and heat transfer. In addition, this study will also infer the optimal configuration of MRAFs on radial fin-tube heat exchangers.

II. THEORY

A. Mathematical Analysis of Fluids Flow and Heat Transfer Performance

The equation governing the fluid flow phenomenon is the mathematical statement of the conservation law of physics which defines fluid as continuity, the rate of change of momentum equal to the force sum of the fluid particle, and the rate of energy change equal to the sum of the incoming energy with energy coming out of the fluid particle. The equations for continuity, momentum, and energy are written in the following tensor form in (1)-(3) [5-6].

$$\frac{\partial u_i}{\partial x_i} = 0 \tag{1}$$

$$\rho \frac{\partial}{\partial x_j}\left(u_i u_j\right) = -\frac{\partial P}{\partial x_i} + \mu\left[\nabla^2 T\right] \tag{2}$$

$$\rho c_p \frac{\partial}{\partial x_j}\left(u_j T\right) = k\left[\nabla^2 T\right] \tag{3}$$

Furthermore, to evaluate the heat transfer on the radial tube fin HE the local Nusselt number is defined as follows (4).

$$Nu = D_0 \frac{\partial\left(\dfrac{T - T_w}{T_b - T_w}\right)}{\partial y} \tag{4}$$

Where D_0 is the diameter outside tube and T_b is the fluid bulk temperature obtained from the following (5).

$$T_b = \frac{\int_A T \mid \rho\vec{v}.d\vec{A}\mid}{\int_A \mid \rho\vec{v}.d\vec{A}\mid} \tag{5}$$

As for the average Nusselt number is based on the surface of the tube whose equations are written as follows (6).

$$\overline{Nu} = \frac{\int Nu \, dA}{\int dA} \qquad (6)$$

The calculation of fin efficiency can simply be written as follows (7).

$$\eta_{fin} = \frac{2}{[1-\left(\frac{u_e}{u_b}\right)^2]} \cdot \left[\frac{I_1(u_b) - \beta.K_1(u_b)}{I_0(u_b) - \beta.K_0(u_b)}\right] \qquad (7)$$

I_0, I_1, K_0, and K_1 are Bessel functions (8),

$$\beta = \frac{I_1(u_e)}{K_1(u_e)}, u_b = \frac{m}{\left(\frac{D+2l}{D}-1\right)}, u_e = u_b\left(\frac{D+2l}{D}\right) \qquad (8)$$

m defined (9),

$$m = I\sqrt{\frac{h}{K.\frac{t}{2}}} \qquad (9)$$

So the total fin surface efficiency is (10)-(12),

$$\eta_{tot} = \frac{1 - \eta_{fin}.A_{fin}.(1-\eta_{fin})}{A_{tot}} \qquad (10)$$

$$A_{fin} = \pi\{(D+2l)t + 0.5[(D+2l)^2 - D^2]\} \qquad (11)$$

$$A_{fin} = \eta_{fin}\pi\{(D.s)(D+2l)t + 0.5[(D+2l)^2 - D^2]\} \qquad (12)$$

Total fin area increases with height fifth change but correlates to decreasing total fin efficiency. The equations for volume for single fin and total heat transfer are as follows (13)-(14).

$$V_{fin} = \pi\left[\frac{(D+2l)^2 - D^2}{4}\right] \qquad (13)$$

$$\dot{Q} = \eta_{tot}A_{tot}h(T_t - T_a) \qquad (14)$$

B. Turbulence Model of RNG k-ε

RNG k-ε is a turbulence model derived from instantaneous Navier-Stokes equations using a mathematical technique called "renormalization group" (RNG) methods. This is the development of the k-ε standard that enhances the accuracy of calculations for the case of strained flow, swirling flow, low Re with viscosity effect and proper treatment in the near-wall region. In addition, the RNG k-ε also provides an analytical formula for the turbulent Prandtl number.

The equations for turbulence kinetic energy (k) in RNG k-ε turbulence model are as follows in (15) [8].

$$\frac{\partial(u_j k)}{\partial x_j} = \frac{\partial\left(\alpha_k \mu_{eff} \frac{\partial k}{\partial x_j}\right)}{\partial x_j} + \frac{\tau_{ij}\partial u_j}{\rho \partial x_j} - \varepsilon \qquad (15)$$

While the equations for turbulence dissipation rate (ε) in (16),

$$\frac{\partial(u_j \varepsilon)}{\partial x_j} = \frac{\partial\left(\alpha_\varepsilon \mu_{eff} \frac{\partial \varepsilon}{\partial x_j}\right)}{\partial x_j} + C_{\varepsilon 1}\frac{\varepsilon}{\kappa}\frac{\tau_{ij}\partial u_j}{\rho \partial x_j}$$

$$- C_{\varepsilon 2}\frac{\varepsilon^2}{\kappa} - R \qquad (16)$$

and equations for energy in (17),

$$\frac{\partial(u_j c_p T)}{\partial x_j} = \frac{1}{\rho}\frac{\partial}{\partial x_j}\left[\alpha_T\left(\mu_{eff}\frac{\alpha T}{\alpha x_i}\right)\right]$$

$$+ \frac{1}{\rho}\frac{\partial}{\partial x_i}\left[\mu_{eff}\left(\frac{\partial u_i}{\partial x_j} + \frac{\partial u_j}{\partial x_i}\right)\right] \qquad (17)$$

Cp is specific heat and T is the time average temperature. Furthermore, the effective viscosity (μ_{eff}) in (15)-(17) is calculated using the following (18).

$$\mu_{eff} = \mu\left(1 + \sqrt{\frac{c_\mu}{\mu}\frac{k}{\sqrt{\varepsilon}}}\right)^2 \qquad (18)$$

μ is a molecular dynamic viscosity. Then turbulent shear stress in equations (15) and (16) is obtained from the following equation.

$$\tau_{ij} = -\rho\overline{u_i' u_j'} \qquad (19)$$

Superscript (') shows fluctuation values and u is velocity. While to solve R in (16) is as follows (20)-(21).

$$R = \frac{c_\mu \eta^3\left(1 - \frac{\eta}{\eta_0}\right)\varepsilon^2}{1 + \beta\eta_3 k} \qquad (20)$$

Where,

$$\eta = \frac{sk}{\varepsilon} \qquad (21)$$

Constant values in governing equation include C = 0.085; $C_{\varepsilon 1}$ = 1.42; $C_{\varepsilon 2}$ = 1.68; η_0 = 4,38; and β = 0.012. While the mean rate modulus of the tensor strain (S) is defined as follows (22)-(23).

$$S = \sqrt{2S_{ij}S_{ij}} \qquad (22)$$

Where,

$$S_{ij} = \frac{1}{2}\left(\frac{\partial u_i}{\partial u_j} + \frac{\partial u_j}{\partial u_i}\right) \qquad (23)$$

The k-ε RNG model provides an accurate description of how effective turbulent transport varies with effective Reynold number. The coefficient α_k, α_ε and α_T in (15)-(17) are the inverse effect of Prandtl number for k, ε, and T. This can be obtained from the following formula.

$$\frac{\mu}{\mu_{eff}} = \left(\frac{\alpha - 1,3929}{\alpha_0 - 1,3929}\right)^{0,6321}\left|\left(\frac{\alpha - 2,3929}{\alpha_0 - 2,3929}\right)\right|^{0,3679} \qquad (24)$$

169

Where, α_0 is 1 / Pr; 1.0; and 1.0 to calculate α_T, α_k, and α_ε. Furthermore, in the near wall zone, the k-ε RNG model is combined with enhanced wall treatment. It aims to divide the domain as a whole into the viscosity affected region and fully turbulent region so that the viscous layer near the wall can be completed accurately. This method requires some consideration of the mesh that the cell adjacent to the wall must be sealed with the parameter $y^+\leq 1$. The equation for calculating y^+ is presented as follows (25)-(26).

$$y^+ = \frac{\rho u_\tau y}{\mu} \tag{25}$$

Where,

$$u_\tau = \sqrt{\frac{\tau_w}{\rho}} \tag{26}$$

The more y^+ close to 1, the calculation for the viscous sublayer will be more accurate so that the convective heat transfer coefficient obtained can approach the experiment. From the simulation model of turbulence that has been done in transitional flow case, RNG k-ε model shows good calculation accuracy compared with SKE Model [8]. Therefore, the RNG k-ε model with enhanced wall treatment will be used in this study to calculate data fundamentals such as air flow and heat transfer on HE radial fin tubes.

C. Boundary Condition

This study, the object used was radial fin tube HE with MRAFs. This will be evaluated using CFDs to obtain the optimal configuration of MRAFs. The radial fin tube HE configuration with MRAFs is described in Figure 1. Furthermore, the detail dimensions for the simulation is written in Table I [9].
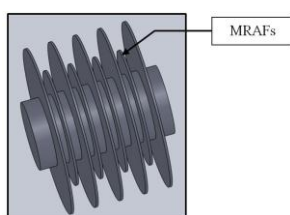

Fig. 1. Radial fin tube HE with MRAFs.

As for the geometry dimensions relevant to the parameters that have been written in Table I illustrated in Figure 1.

The method used in this research is numerical analysis in 3D with CFD code Fluent. The procedures are pre-processing, processing (input value boundary condition and solver determination), and post-processing. The research stages will be described as follows.

Stages of this process consist of geometry, meshing, and boundary condition determination using Gambit 2.4.6 software. The geometry design is carried out using the data already described in figure 2 (a), the fluid flow zone is divided into 3 regions as illustrated in Figure 2 (b). Region A with dimensions x = 8D, y = 8, and z = 1.6D; Region B with dimensions x = 2D; and Region C with dimensions x = 20D. The pre-formed geometry is then processed for the mesh

surface by assigning nodes to each line. In this process, discretization near the tube is more than the others. This serves to avoid miscalculation to obtain accurate results with a relatively small number of cells. The mesh surface used is a quadrilateral map. The mesh surface used in this study is illustrated in Figure 3.

TABLE I. Dimension of radial fins tube HE and MRFAs.

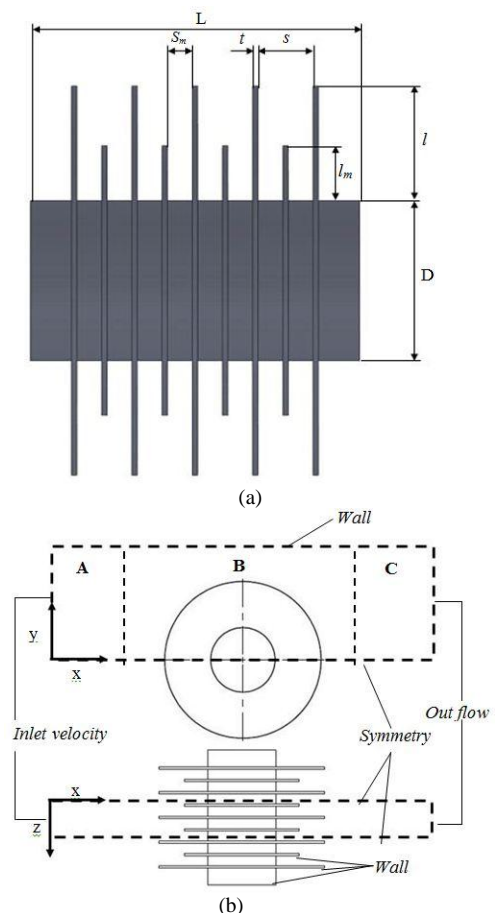| Cylinder	Dimension
Length (L), mm	120
External diameter (D), mm	78
Fins	
spacing (s), mm	20
height (l), mm	35
Thickness (h), mm	2
MRAFs	
spacing (s_m), mm	9
height (l_m), mm	5, 10, 15, 20, and 25
Thickness (h_m), mm	1, 1,5, and 2

(a)

(b)

Fig. 2. Radial fin tube HE with MRAFs: (a) geometry and (b) boundary condition on computational domain.

After designing geometry and meshing, a further determination of the boundary condition as illustrated in Figure 2 (b). Boundary condition serves to determine the boundary conditions required for the simulated object in accordance with the conditions of use. Furthermore, the downstream is determined as an outflow because the flow is conditioned fully developed flow so that the results obtained more accurately, towards z of the domain are assumed to

reduce symmetry of the same domain so as to accelerate iteration, and tube is defined as wall because the heat transfer process occurs in constant wall temperature. The results from Gambit are then exported in the form of a mesh which is then used for the simulation process in Fluent software.
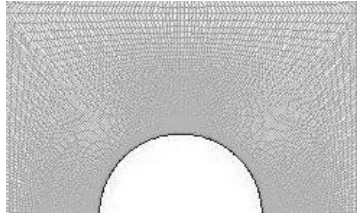

Fig. 3. Mesh surface.

This process is done in Fluent 6.3.26 software in the form of the value of every boundary condition specified in Gambit will be input. In detail, the values are listed in Table II. The turbulence model used is k-ε RNG by activating enhancement wall treatment in the form of pressure gradient and thermal effects. The fluid used is incompressible air with constant properties. The air properties shown in Table II. The assumption used in the form of 3D turbulence flow, uniform, steady, no viscous dissipation, and the effects of radiation are ignored. For streamwise gradient (Neumann boundary condition) in all variables is 0. On tube wall specified a no-slip condition and constant wall temperature with material and its properties are shown in Table III. Pressure-velocity coupling is completed using SIMPLEC with discretization for pressure, momentum, turbulent kinetic energy, turbulent dissipation energy, and energy are second-order upwind. As for the under-relaxation factor is the default user value. Convergence criterion used in the simulation for all variables is 1.0×10^{-5}. After the iteration process is done and in accordance with the boundary convergence criterion, then do post-processing for data that has been obtained.

TABLE II. Value of boundary condition.

Boundary condition	Value
Inlet	Tipe = Velocity inlet V_{in} = 5 m s^{-1} T_{in} = 27 ^{0}C
Outlet	Outflow
Radial fin tube	Stationary wall T_w = 80 ^{0}C Material copper
MRAFs	Stationary wall
line	Symmetry

TABLE III. Properties of air and copper.

Parameter	Properties	Value
Air	Density (kg m^{-3})	1,1614
	Specific heat (kJ kg^{-1} K^{-1})	1,007
	Absolute viscosity (kg m^{-1} s^{-1})	1,846x10^{-5}
	Thermal conductivity (W m^{-1} K^{-1})	0,0263
Copper	Thermal conductivity (W m^{-1} K^{-1})	387,6

The result of the later iteration process is extracted from data to be processed and evaluated. The data to be processed quantitatively is Nu_m. While qualitatively is the visualization of flow and temperature distribution across the radial fin tube HE with MRAFs. Overall quantitative data will be processed using Tecplot 360 software to obtain Nu_m distribution so it can be displayed in graphical form for analysis.

III. RESULT

A. Grid Independency Test and Numerical Validation

In studies using numerical methods, grid-independence tests should be performed to ensure the accuracy and validity of the numerical results. Therefore, in this study the grid-independence test was conducted at 2D baseline condition with parameters such as D = 12.7 mm, P_L = 2.17D, P_T = 2.48$_D$, and Re_D = 4000.
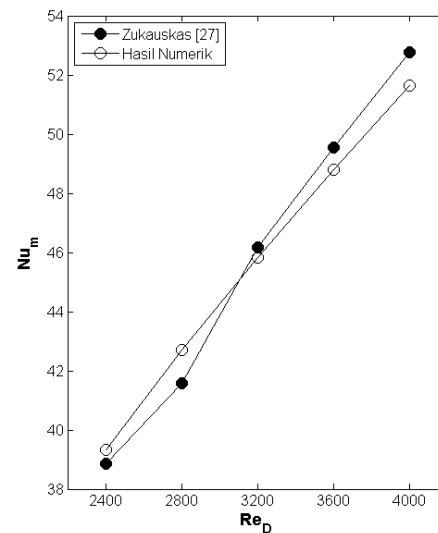

Fig. 4. Numerical validation.

From the grid-independence test in Figure 4, it can be seen that by varying the number of cells near the wall, the y + ≤l approach, can improve the accuracy of the calculations. A relatively small error is shown in mesh B with a percentage of 2% compared to empirical correlation. Furthermore, the validity study of B mesh was developed in the form of a comparison between Nu_m numerical results and experiments on each variation of Re_D. The results shown in Figure 4 describe that the maximum deviation between the numerical and experimental results is 2% at Re_D = 4000 and the minimum deviation of 0.7% at Re_D = 3200. Therefore, mesh B can be categorized as good and feasible to be used as a reference in the determination of the grid number in the case of radial fin tube HE with and without MRAFs in 3 dimensions.

B. Average Nusselt Number with Height and Thickness Variations of MRFAs

The simulation result using Fluent software is shown in Figure 5. In the l_m variation with h_m 1 mm it shows that the greater the value of Nu_m is smaller. The same graph trend is also shown in the variation of h_m 1.5 mm. This is due to the influence of secondary flow separation of 3D from the flow through the narrow gap on h_m 1. The separation effect contributes to the fluctuation of heat and flow (blockage effect) through the fin gap. The bigger the lm the secondary
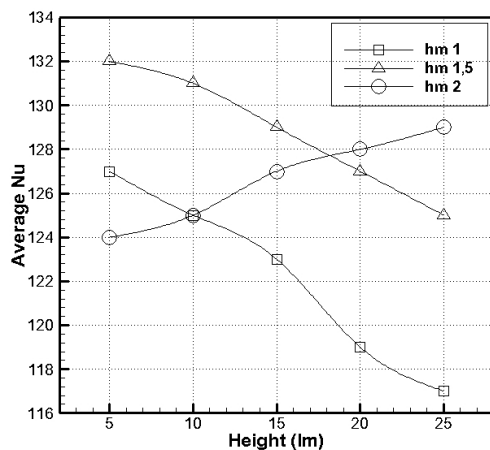
flow effect gets bigger so Nu_m gets smaller.

Fig. 5. Nu_m vs. h_m and l_m MRFAs.

A different phenomenon is shown in the variation of h_m 2 mm the greater l_m, the greater the Nu_m. This is because the secondary flow effect affects the delay of the separation layer on the surface of the tube. The delay of the separation layer on the surface of the tube contributes to the depletion of the thermal boundary layer so that Nu_m gets bigger. In addition, the greater the gap hm, blockage effect is reduced so that the flow of freestream the better.

When viewed from the value of Nu_m then can be obtained the use of MRAFs on radial fins is the optimal combination of l_m 5 mm with h_m 1.5 mm. However, when compared with the baseline showed a significant decrease of 0.41%. This is due to the effect of narrowing the flow area of the free stream by MRFAs, secondary flow 3D, and blockage effect.

IV. CONCLUSION

The conclusions are written in the progress report as follows.
a. The use of MRAFs has a significant effect on the flow turbulence across the fins gap. The narrowness of MRFAs with flow turbulence fins is increasing. However, increased flow affects the occurrence of secondary flow separation that inhibits heat transfer. This is indicated the smaller the hm and the larger lm, the less Num.
b. The optimal configuration of the use of MRAFs in the radial fin tube HE is 5 mm by 1.5 mm.

REFERENCES

[1] Dong-Kwon Kim, "Thermal optimization of branched-fin heat sinks subject to a parallel flow," *Int. J. of Heat and Mass Transfer*, vol. 77, pp. 278–287, 2014.
[2] Haleh Shafeie, Omid Abouali, Khosrow Jafarpur, and Goodarz Ahmadi, "Numerical study of heat transfer performance of single-phase heat sinks with micro pin-fin structures," *Applied Thermal Engineering*, vol. 58, pp. 68-76, 2013.
[3] H. E. Ahmed, "Optimization of thermal design of ribbed flat-plate fin heat sink," *Applied Thermal Engineering*, 2016.
[4] Ramadan Bassiouny, Hisham Maher, and Adel A. Hegazy, "On the thermal analysis of a plate-fin heat sink considering the thermal-entry length effect," *Applied Thermal Engineering*, 2016.
[5] Ivano Petracci, Luca Manni, and Fabio Gori, "Numerical simulation of the optimal spacing for a radial finned tube cooled by a rectangular jet-average thermal results," *Int. J. of Thermal Sci.*, vol. 104, pp. 54-67, 2016.
[6] Li Zhang, Wenjuan Du, Jianhua Wu, Yaxia Li, and Yanwei Xing, "Fluid flow characteristics for shell side of double-pipe heat exchanger with helical fins and pin fins," *Experimental Thermal and Fluid Science*, vol. 36, pp. 30–43, 2012.
[7] L. J. Li, C. X. Lin, and M. A. Ebadian, "Turbulent mixed convective heat transfer in the entrance region of a curved pipe with uniform wall temperature," *Int. J. Heat and Mass Transf.*, vol. 41, pp. 3793-3805, 1998.
[8] Si-Min Huang, Minlin Yang, Yu Yang, and Xiaoxi Yang, "Fluid flow and heat transfer across an elliptical hollow fiber membrane tube bank for air humidification," *Int. J. Thermal Sci.*, vol. 73, pp. 28-37, 2013.
[9] Masao Yoshida, Sochi Ishihara, Yoshio Murakami, Kohei Nakashima, and Masago Yamamoto, "Air cooling effect of fins on a motorcycle engine," *JSME International Journal B*, vol. 49, pp. 869-875, 2006.